Reactive Scattering of 1−5 eV O^- in Films of Tetrahydrofuran

Michael A. Huels,* Luc Parenteau, and Léon Sanche†

Department of Nuclear Medicine and Radiobiology, Faculty of Medicine, University of Sherbrooke, Sherbrooke, Québec, Canada J1H 5N4

Received: June 16, 2004; In Final Form: August 4, 2004

An understanding of *all* nascent events leading to radiolytic DNA damage is required to achieve a complete description of ionizing radiation effects on living cells. These early, subpicosecond events involve mainly low-energy ($E < 20$ eV) secondary electrons (SE) and low-energy ($E < 5$ eV) secondary ion (and neutral) fragments; the latter are created either by the primary radiation or by SE via resonant mechanisms, i.e., dissociative electron attachment (DEA). While recent work has shown that 3−15 eV SE *initiate* DNA strand break formation exclusively via resonances, the subsequent damage induced by the energetic DEA ion fragments in DNA or its basic components is unknown. Here, we report 0−20 eV electron impact measurements of negative ion desorption from condensed films containing O_2 and tetrahydrofuran, C_4H_8O (THF), a deoxyribose analogue. Our experiments show that all of the OH^- and some of the H^- desorption yields are the result of reactive scattering of the 1−5 eV O^- fragments produced initially by DEA to O_2. These O^- reactions involve hydrogen abstraction and atom exchange from THF, and result in the formation of THF-yl radicals, as well as THF oxidation products, most likely lactones and alkoxyl radicals. O^- scatters over nanometer distances comparable to DNA dimensions, and reactions involve formation of a transient $(OC_4H_8O)^{*-}$ collision complex. Our measurements support the notion that in DNA, exposed to ionizing radiation, similar localized secondary ion reactions can be *initiated* by the abundant secondary electrons, and may result in further clustered damage, lethal chemical transformations, and enhance DNA lesions.

Introduction

Although radiation therapy is a frequent mode of cancer treatment, the complex sequence of events that leads to radiation damage of cellular DNA is still not fully understood. Much of the uncertainty concerns the nascent reaction cascades that unfold on subpicosecond time scales after the interaction of ionizing radiation with living tissue. When such radiation, particularly heavy ions, deposits energy in matter it produces abundant nonthermal ions, neutral radicals, and ballistic secondary electrons (SE is about 5×10^4/MeV deposited[1]). The majority of the latter have initial kinetic energies between 1 and 20 eV,[1−3] and efficiently induce additional production of energetic (1−5 eV) anion fragments via formation of dissociative anion states (resonances), i.e., dissociative electron attachment (DEA),[4] which also occurs on short time scales ($\leq 10^{-13}$ s). This has been shown to be the case for most DNA/RNA components,[5] e.g., deoxyribose analogues,[6] DNA bases,[7−10] uracil,[8,11] water ice,[12] amino acids,[13,14] single stranded oligonucleotides,[15] and even double stranded plasmid DNA.[16] For thymine and cytosine, for example, DEA anions include OCN^-, CN^-, H^-, O^-, and their associated neutral radical fragments, while many other types of anion fragments are produced by DEA to the other targets. In cells, all of the initial energetic transients (SE, ion and radical fragments) formed along radiation tracks will thermalize within 10^{-12} s via multiple inelastic interactions with their environment; this may lead to important physical and chemical modifications of the medium, prior to all the subsequent diffusion-limited chemical damage that occurs at later times. Thus, a detailed knowledge of these nascent reactions, and their products, is essential in order to establish the link between the physicochemical (10^{-15}−10^{-12} s) and chemical (10^{-12}−10^{-6} s) stages of cellular radiolysis.

While recent studies have revealed the surprising efficiency of 3−20 eV secondary electrons to induce DNA damage via DEA, i.e., formation of nonthermal anion and radical fragments within DNA, the subsequent reactive damage induced by these fragments in DNA is unknown. More specifically, we have found that (a) 3−15 eV electrons initiate the formation of high yields of single (SSB) and double (DSB) strand breaks in double-stranded supercoiled DNA (plasmids) *exclusively* via resonance mechanisms[17,18] and (b) these resonant strand breaks are notably associated with formation and desorption of energetic H^-, O^-, and OH^-, via DEA within the plasmids.[16] DEA to a specific DNA component may itself generate *one* SSB; however, we also observe formation of DSB[17] at electron energies well below those required for *two* SSB, i.e., two successive ionizations ($\gg$12 eV)[19] by a single electron, to occur within 10 base pairs of each other on opposing phosphate−sugar strands. This suggests that *the resonant formation of DSB by a single electron involves subsequent reactions of energetic DEA fragments*, which lead to a doubly damaged site with breaks on opposing strands, and which immediately raises two questions: (a) what type of damage can these nonthermal DEA anion fragments induce by reactions with DNA components and (b) over what distances from their original formation site may such reactions take place before the energetic anions are sufficiently attenuated, and are no longer able to reach the opposing DNA backbone. These points we intend to address here.

A priori, all of the anion fragments produced by DEA to any DNA component may be involved in subsequent reactive

* To whom correspondence should be addressed. E-mail: michael.huels@usherbrooke.ca.

† Canadian Research Chair in the Radiation Sciences.

10.1021/jp047385i CCC: $27.50
Published on Web 09/22/2004

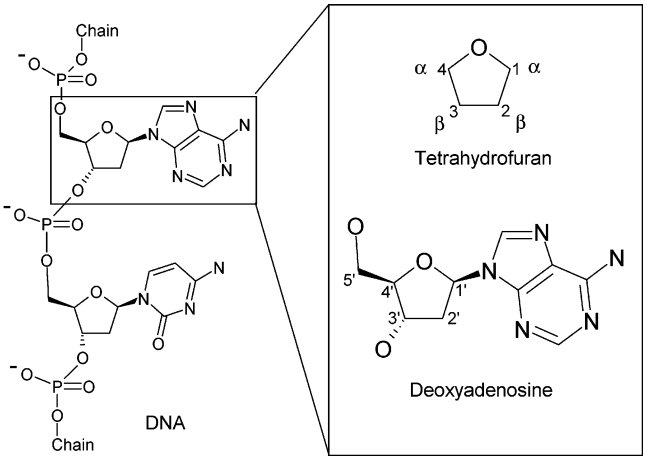

Figure 1. Structure of tetrahydrofuran (THF), a nucleoside, and small section of DNA; the complementary strand is not shown for clarity.

damage; however, so far only H^-, O^-, and OH^- have been observed to be formed by SE in both films of DNA *and* some of its components with sufficient kinetic energy to overcome the charge-induced polarization barrier (near 1 eV for hydrocarbon films[20]) near the surface and desorb, to be measured by a mass spectrometer. Among these ions, only O^- is a reactive radical anion, and it is therefore our first choice to study post-DEA ion reactions with components of DNA in the condensed phase. Because of the energies involved in these *nonthermal* ion reactions, they cannot be classified as "ordinary" chemical reactions; they occur on a much faster time scale (10^{-14}−10^{-12} s) and are highly inhomogeneous. Reactive scattering of low-energy (<5 eV) atomic (or molecular) anions with atoms and molecules is well explored in the gas phase even at near thermal collision energies,[21] yet only a few such studies exist in the condensed phase. Reactions of energetic O^- in condensed films were first noted in the electron-stimulated desorption (ESD) yields from O_2 embedded in multilayer films containing simple alkenes or alkanes[20,22,23] or aniline,[24] and in $^{18}O_2/C^{16}O$ mixed solids.[25] Part of the H_2 ESD yield observed from multilayer films of H_2O, at electron energies below 10 eV, has also been attributed to proton abstraction by DEA H^- fragments,[26] viz., $H^- + H_2O \rightarrow \{H_3O\}^{*-} \rightarrow H_2 + OH^-$, and has been associated with part of the unscavengeable H_2 yield formed in water radiolysis.[27] Finally, as noted by Madey and co-workers,[28] the in situ production of reactive 1−10 eV ions by electron impact at surfaces is an effective method to investigate low-energy ion scattering and attenuation in condensed overlayers.

Here we present measurements of O^- reactions in physisorbed films of tetrahydrofuran (THF, C_4H_8O), a DNA sugar analogue, initiated in situ by 0−20 eV electron impact in films containing both THF and O_2. The latter merely serves as a source of O^- with well characterized kinetic energy distributions in the 1−5 eV range.[29] The choice of THF is based on its structural similarity to the deoxyribose backbone in DNA, shown in Figure 1, and is used here as a model compound to qualitatively estimate damage to these specific DNA sites induced by DEA anion fragments. We note that in DNA hydrogen abstraction from the C4′ (or C3′) site will lead to a single strand break[30] by phosphate elimination at C5′ or C3′, while CH bond rupture at the C1′ position may lead to base loss. To the best of our knowledge, no studies exist to date on the physicochemical consequences of nonthermal ion reactions with DNA, or its components and analogues, particularly at collision energies below the electronic excitation threshold of the target (below 6 eV for THF[31]). Here we show that at least two O^- reaction channels, namely hydrogen abstraction (OH^- formation) and reactive charge transfer (atom exchange), are energetically possible for 1−5 eV O^-. Our measurements furthermore support the notion that, at the small impact parameters dictated by the condensed phase, the O^- + THF reactions proceed via formation of a $(O-THF)^{*-}$ transition state (or collision complex) that may decay along numerous energetically allowed pathways, similar to gas-phase anion reactions.[21] In the following sections we present the experimental method and results and summarize the radiobiological relevance of the reactions observed here.

Experimental Method

The apparatus and methods used in the present investigation have been discussed in great detail elsewhere,[22,29,32] and only a brief description is given here. A monochromatic electron beam of about 2 nA, or less, with incident energies between 0 and 20 eV, and a resolution of about 100 meV, impinges at 70° from the surface normal onto a thin polycrystalline Pt foil press-fitted directly onto the tip of a closed cycle cryostat. The Pt foil is held at about 20 K during the sample preparation and experiments, and is cleaned by resistive heating to 1000 K. This procedure results in a reconstructed polycrystalline Pt surface whose microcrystals have azimuthal disorder with a (111) orientation.[33] Multilayer films are condensed on the clean Pt by means of a volumetric dosing procedure,[34] with an accuracy of about ±30% and an overall repeatability of ±0.2 monolayers (ML). Pure O_2 condensed on this Pt substrate is well known to form nonporous amorphous solids, with rough surface structure.[29a,b]

Some of the negative ions produced under electron impact may desorb and enter an ion lens system (containing a system of retardation grids) that precedes a quadrupole mass spectrometer (QMS), positioned at 90° from the incident electron beam, and operating in a standard pulse counting mode. The QMS system may be operated in the *ion yield* mode, where the signal of a particular desorbing anion species is monitored as a function of incident electron energy, E(e), or the *ion energy* mode, where the anion signal is recorded versus the retardation voltage on the grids, at a fixed E(e) and ion mass-to-charge ratio. The geometry of the QMS ion optics and the target is such that all measurements presented here are (desorption) *angle integrated* over a solid angle of about 50° width, centered on the principal axis of the QMS.[29]

The minimum purity (as purchased) of the compounds used is 99+% (tetrahydrofuran (C_4H_8O), THF) and 99.998% for O_2, respectively. The THF is furthermore purified in-house by a number of freeze−pump−thaw cycles. The experiments are performed in a standard UHV chamber, with a base pressure of 10^{-10} Torr, which is enveloped by two layers of μ-metal shielding. All measurements are obtained immediately after sample preparation to minimize contamination of the surface by background gases. The measured anion yield functions contain an estimated experimental uncertainty of about 12%, and are repeatable to within 5%. The absolute E(e) scale is determined to within ±0.15 eV of the vacuum level (here $E_{vac} \equiv 0$ eV) by observing the onset of current transmission through the condensed film[35] as a function of E(e). Since energy shifts of this onset determine the amount of charging of the films, it is possible to verify that all results presented here are obtained under charge-free conditions.

Results and Discussion

Shown in Figure 2 are the ESD yields of anions which desorb under 0−20 eV electron impact from homogeneous O_2, or THF

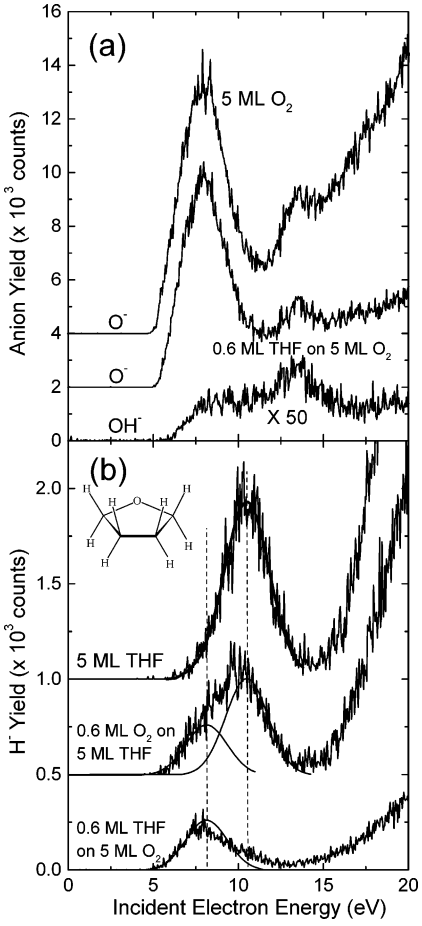

Figure 2. Electron-stimulated desorption (ESD) yields of O^-, OH^-, and H^- from pure and mixed films of O_2 and THF, all as functions of incident electron energy from 0 to 20 eV. In both panels a and b the yield curves have been displaced vertically for clarity. Other than film composition, experimental conditions were identical for all films. In panel a we show ESD yields of O^- from a five monolayer (ML) film of pure O_2 (top curve), and from a film of 0.6 ML of THF on 5 ML of O_2; for the latter film the OH^- yield is also shown (multiplied by 50). In panel b we show ESD yields of H^- from a pure 5-ML film of THF (top curve), from 0.6 ML of O_2 on 5 ML of THF, and from 0.6 ML of THF on 5 ML of O_2 (bottom curve). The smooth Gaussian curves superimposed on the data in panel b are described in the text (next section), and their approximate energy positions are indicated by the dashed vertical lines; the structure of THF is also indicated in panel b.

films, as well as various types of heterogeneous films containing both O_2 and THF; these will be discussed in the following three sections.

ESD from Homogeneous Molecular Films. The double peak ESD signature of the O^- yields from a 5-ML film of pure O_2 (top curve in Figure 2a) is the result of DEA to condensed phase O_2, which has been described in great detail elsewhere;[29,32,36] here we outline DEA to O_2 to briefly emphasize the differences between the gas and condensed phases relevant to the present discussion.

In addition to the well-known $^2\Pi_u$ gas-phase resonance observed at 6.7 eV, previous experiments have demonstrated that DEA to physisorbed O_2 also involves gas-phase forbidden transitions to Σ^+ states of O_2^-,[37] i.e.

$$e^- + O_2(^3\Sigma_g^-) \rightarrow O_2^{*-}(^2\Pi_u, {}^2\Sigma_u^+, {}^2\Sigma_g^+) \rightarrow O^-(^2P) + O(^3P \text{ or } {}^1D) \quad (1)$$

This leads to O^- formation peaks at E(e) near 8−9 and 13.5 eV, as shown in the top curve in Figure 2a, superimposed on a monotonically rising O^- signal that is usually attributed to *direct* dipolar dissociation (DD) at higher E(e), i.e.

$$e^-(E) + O_2 \rightarrow O_2^{**} + e^-(E' < E) \rightarrow O^- + O^+ + e^-(E' < E) \quad (2)$$

Direct DD is a *nonresonant* ion pair formation mechanism, with a threshold of 17 eV for O_2. However, electron energy loss (EEL) to O_2 followed by DEA (to the low-lying O_2 resonances) also occurs at E(e) above 11 eV, and has been shown to dominate the O^- ESD yields at higher electron energies.[38]

In the condensed phase, the ionic (or neutral) fragments created by DEA (or DD) may either desorb or remain at the surface, or in the bulk, of the solid. Anions that remain may either be trapped[39] by the charge-induced polarization energy (E_p) of the solid or react with their environment.[22,25] The DEA fragments which desorb possess kinetic energies $E_k > E_p$; for condensed-phase O_2, and at $5 < E(e) < 15$ eV, the in vacuo kinetic energy distributions of O^- from DEA to O_2 are generally characterized[29] by (1) a most probable kinetic energy, E_k(mp), that varies between 0.25 and 3 eV and (2) a maximum possible kinetic energy, E_k(max), that varies between 1 and 5 eV. Thus, near the surface (prior to desorption or reactions) the O^- kinetic energies are larger by an average E_p (0.4−0.7 eV for the disordered O_2 films condensed here at 20 K[29a]). Further ESD measurements from O_2 adsorbed on thick CH_4 and C_2H_6 substrates[40] show that the O^- E_k distributions are not strongly affected by the presence of these hydrocarbons, other than the slightly higher average E_p (≈1 eV for hydrocarbons[20]).

Anion ESD from pure THF films has been discussed in great detail elsewhere;[6] for E(e) < 40 eV it leads *exclusively* to desorption of H^- with a strong resonance peak near 10.5 eV, as shown in the top curve in Figure 2b. Thus, for E(e) below 20 eV, the desorption of O^- and OH^- from THF coadsorbed with O_2 is *not* due to interactions of electrons with the THF. The broad DEA H^- peak in THF films near 10.5 eV has been attributed mainly to α-CH bond cleavage via a core excited shape resonance, and results in desorption of H^- with in vacuo E_k(mp) near 0 eV and E_k(max) near 4 eV. DEA via α-CH bond rupture is believed to be favored over β-CH sites, due to the influence of the directly attached oxygen heteroatom. For pure THF films, the steeply rising H^- signal above 15 eV (Figure 2b, top curve) has been attributed to a combination of EEL followed by DEA, direct DD, as well as electron autodetachment of a 6 eV broad, core-excited valence-type resonance near 23 eV (involving the furan ring) into electronically excited DD-like states of neutral THF. Finally, we note that multilayer films of most linear and cyclic hydrocarbons (but *not* O_2) are known to form amorphous *porous* films when condensed at 20 K; this allows small molecules such as O_2 to enter the pores of such hydrocarbon substrates.[41] Amorphous *nonporous* or crystalline hydrocarbon films are formed either by annealing or by directly condensing the films at higher temperatures (usually between 60 and 100 K). For such nonporous hydrocarbon films (e.g., benzene) cooled to 20 K, molecules such as O_2 have been shown to reside exclusively at the surface.[41]

Reactive Scattering of O^- in Heterogeneous Films. Shown in Figure 2a are the O^- and OH^- ESD yields from a 5-ML film of O_2 when about 0.6 ML of THF has been deposited at the surface. Although here the O^- yield at 20 eV is somewhat reduced relative to the intensities at the two peaks,[42] we find that the overall resonance signature of DEA to O_2 is essentially unchanged relative to a pure O_2 film (as are the KE distributions of O^- from DEA[40]). Furthermore, the O^- ESD signature seen here for 0.6 ML of THF on O_2 essentially remains the same for

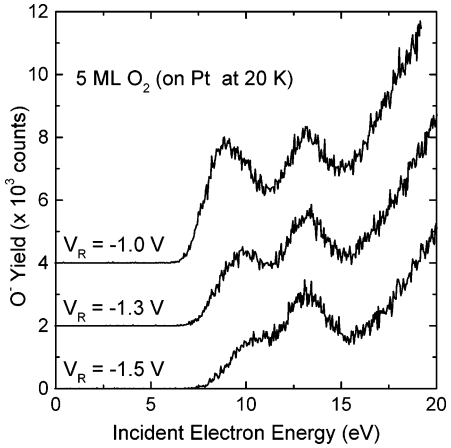

Figure 3. ESD yields of O^- from 5 ML thick films of pure O_2, all as functions of incident electron energy from 0 to 20 eV, and for three different retardation voltages (V_R) applied to the grids contained in the lens system preceding the quadrupole mass spectrometer (QMS). The curves have been vertically displaced for clarity, and all experimental conditions (except V_R) were identical.

THF coverages up to about 8.7 ML (however, the intensity decreases due to attenuation of the desorbing O^-; this will be shown in the next section). Thus, DEA to O_2 does not appear to be significantly affected by the presence of THF. However, for THF adsorbed on O_2 films, we also observe desorption of OH^- under electron impact, with a typical double peaked desorption signature as that shown in Figure 2a. We also note the following: (1) since ESD from pure THF films[6] does not yield O^- or OH^-, here they do not arise from electron interactions with THF, (2) the OH^- signal increases linearly with THF surface coverage below 1 ML, and (3) the OH^- yield signatures more closely resemble the yield function of those O^- that desorb from pure O_2 films with in vacuo $E_k \approx 1.0$ eV or more (i.e., the O^- yields measured with a 1.0 V potential on the retardation grids), than the H^- signal associated with DEA to THF. This point is demonstrated in Figure 3, which shows O^- yields from pure O_2 films for different retardation potentials, V_R, and which closely resemble the OH^- yield signatures observed here. Similar OH^- desorption signatures were seen in previous ESD experiments on mixed films of O_2 and small alkenes or alkanes,[20,22,23] and where the OH^- ESD yield, attributed to O^- reactions with the coadsorbed hydrocarbons, increased linearly with alkane coverage below 1 ML.

Furthermore, the E_k distributions of ESD H^- from THF films do not extend beyond 4 eV,[6] and in gas-phase collisions at energies below 5 eV[43] the only anion product observed in $H^- + O_2$ scattering is $O_2^-(^2\Pi_g)$. Although HO_2 has a positive electron affinity (EA) of about 1 eV,[44] stable HO_2^- cannot be formed in gas-phase $H^- + O_2$ scattering, since the reaction exothermicity cannot be dissipated. Here in the condensed phase, HO_2^{*-} may in principle still be formed (in some predissociative state), since the surrounding medium could absorb some of the exothermicity. However, in that case any OH^- formed by autodissociation of such HO_2^{*-} would bear the signature of H^- formation via DEA (seen in Figure 2b, top curve), which is completely different than the actual OH^- signature observed here.

On the other hand, associative electron detachment (AED), i.e., $H^- + O_2 \rightarrow [HO_2]^{*-} \rightarrow HO_2 + e^-$, becomes active in the gas phase for center of mass collision energies below 2 eV;[43] here, in the condensed phase, one might thus argue that formation of OH^- is predominantly the result of DEA to HO_2 (formed previously by AED) by subsequently arriving electrons. However, the following arguments speak against this: (1) here the incident electron beam flux density is about 10^{11} s^{-1} cm^{-2}, i.e., significantly less than the THF surface density of about 5×10^{14} cm^{-2}, and accumulation of sufficient HO_2 in the film would require irradiation times much longer than those used in the present experiments (about 2−5 min/scan), (2) OH^- desorption is observed here immediately on the first electron energy scan, where the E(e) is scanned from low to high, and (3) the intensity of OH^- ESD is linear in electron beam intensity.

Thus, based on the above experiments and discussions, and previous observations of OH^- ESD in mixed films containing O_2 and linear hydrocarbons,[23] we attribute the present OH^- desorption signal, observed during electron impact to films containing O_2 and THF, to hydrogen abstraction from THF by O^- that are formed initially by DEA to O_2, viz., reaction 1 followed by

$$O^- + C_4H_8O \rightarrow [OC_4H_8O]^{*-} \rightarrow OH^- + {}^{\cdot}C_4H_7O \quad (3)$$

Here the asterisk denotes a transient, possibly excited state. As shown previously, in low energy gas[21] and condensed phase[20,22−25] anion−molecule reactions, such reactive scattering requires the formation of a molecular anion transition state, or collision complex, here formation of $[OC_4H_8O]^{*-}$. The existence of similar transient molecular anion collision complexes has previously been suggested by Comer and Schulz,[45] who measured the energies of electrons emitted during gas-phase collisions of O^- with small hydrocarbons such as C_2H_4. These authors demonstrated that the electron energy distributions were the result of AED, i.e., $O^- + C_2H_4 \rightarrow [OC_2H_4]^{*-} \rightarrow e^- + C_2H_4O$, where OH^- formation via an analogue of reaction 3 was also observed to be a dominant channel. These and many other gas-phase studies[46−48] have shown that low-energy O^- collisions with hydrocarbons proceed via formation of a transient anion collision complex, and result in various reactive scattering products, where hydrogen abstraction is almost always a dominant channel.

We also find that when OH^- formation via reaction 3 is observed during electron impact on 5 ML of O_2 covered with 0.6 ML of THF (Figure 2a), the H^- yield signature from the same film (Figure 2b, bottom curve) is drastically different than that from a 5-ML film of pure THF (Figure 2b, top curve): while formation and desorption of H^- via DEA in pure THF films[6] has a threshold near 6.5 eV and peaks near 10.5 eV, for 0.6 ML of THF on 5 ML of O_2 the H^- desorption signature now has a threshold near 5 eV, i.e., lowered by 1.5 eV, and a peak near 8 eV, while the 10.5 eV H^- peak associated with DEA in pure THF films is absent. Other data (not shown) demonstrate that (a) as the amount of THF on O_2 is decreased below 0.6 ML, this different H^- ESD signature remains constant in shape, however, the 8 eV peak intensity does decreases linearly with THF concentration down to about 0.1 ML of THF, and (b) the 10-eV peak, associated with DEA to THF, only becomes noticeable when the amount of THF on O_2 is increased significantly above 1 ML. Similarly, as shown in Figure 2b (middle curve), when 0.6 ML of O_2 is adsorbed on 5 ML of THF, in addition to the 10.5-eV peak, the H^- ESD yield now has an additional structure near 8 eV, and a desorption threshold near 5 eV. The contribution of this structure to the ESD signature is shown in Figure 4, where the H^- ESD yield from 0.6 ML of O_2 adsorbed on 5 ML of THF (at 20 K) is deconvoluted via the following method: the DEA H^- yield from a pure 5-ML film of THF is fitted with a Gaussian, normalized in intensity at 10.5 eV (G(1) in Figure 4) to the H^- yield from 0.6 ML of O_2 on 5 ML of THF, curve a in Figure 4, and then subtracted from

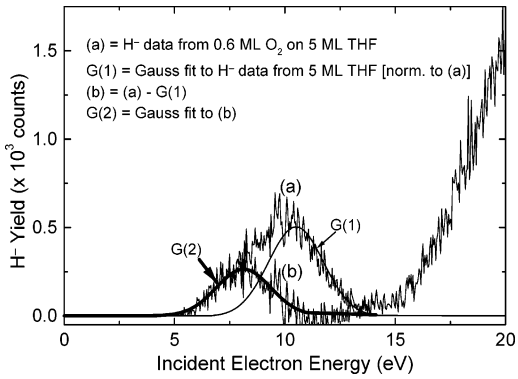

Figure 4. Deconvolution of the H^- ESD yield from 0.6 ML of O_2 on 5 ML of THF (from Figure 2b) as described in the text. Here G(1) (thin line) is normalized in intensity at 10.5 eV to data curve a.

curve a. The remaining data signal after subtraction, curve b, is then fitted with a Gaussian, G(2). Since here the 5-ML THF film is condensed at 20 K, and therefore has porous amorphous structure,[41] much of the adsorbed 0.6 ML of O_2 is likely to reside within the pores of the THF film (experiments with O_2 on crystalline THF films are shown in the next section). These two Gaussians G(1) and G(2) are also shown in Figure 2b superimposed on the data. We note that when G(2) (or curve b), which was extracted from the 0.6 ML of O_2 on 5 ML of THF data, is superimposed without further manipulation on the H^- ESD yield from 0.6 ML of THF on 5 ML of O_2 in Figure 2b they match extremely well, particularly for E(e) below 8 eV. This suggests that, at least for E(e) between 5 and 8 eV, H^- formation and desorption from either of these films is dominated by a process that strongly depends on the presence of O_2. This is furthermore supported by the observation that the main parameters, i.e., electron energy threshold (5 eV), energy width, and peak position (8 eV), of this low-energy process G(2) are in excellent agreement with the ESD signature of O^- formed via DEA to the low energy resonances of O_2 in either the 5-ML films of pure O_2 or O_2 coadsorbed with THF (Figure 2a). In other words, even for small quantities of O_2 coadsorbed with large amounts of THF, in addition to H^- formation via direct DEA to THF (with a threshold near 6.5 eV and peak near 10.5 eV), we now observe evidence for a second process of H^- formation that in fact more closely resembles the energetics of O^- formation via DEA to the lower resonances of O_2 (see Figure 2a). This second process, however, clearly dominates the H^- ESD yield when only small quantities of THF are adsorbed on large quantities of O_2.

Given these observations, the simultaneous formation of OH^- via O^- collisions in these films, and known values of bond dissociation energies[49] (D_o) and electron affinities[50] (EA), we attribute the H^- desorption yield, at incident electron energies near or below the threshold for direct DEA to THF, to reactive scattering of O^- with THF leading to atom exchange. On the basis of general gas-phase anion−molecule interaction dynamics,[21] at the small impact parameters dictated by the condensed phase, such reactions proceed via the same, or similar, transient collision complexes responsible for OH^- production in reaction 3, i.e.

$$O^- + C_4H_8O \rightarrow [OC_4H_8O]^{*-} \rightarrow H^- + OC_4H_7O \quad (4)$$

Since in reaction 3 the motion of the $[OC_4H_8O]$ core during the collision is much slower than that of the *extra* electron in its diffuse orbital, the latter may easily adjust to reactions in the molecular core. Depending on the autodetachment lifetime

SCHEME 1: Some of the Energetically Allowed Reaction Channels Involved in the Decay of $[OC_4H_8O]^{*-}$ Transition States (or collision complex) That Are Formed during 1−5 eV O^- Reactions with THF

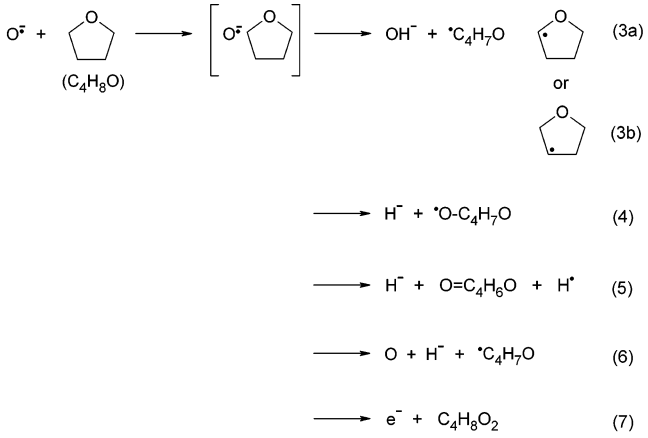

($\approx 10^{-14}$ to 10^{-13} s) and potential energy surfaces of the transient molecular anion complex formed during the collision, several decay channels are available to it, one of which leads to OH^- production as in (3); however, many other decay channels observed in the gas phase may also be possible here, one of which leads to atom exchange via reaction 4. Similar reactions have been observed in ESD experiments on heterogeneous films containing O_2 and small alkanes and alkenes.[23] More specifically, in these experiments, in addition to reactions 3 and 4, O^- reactions with C_2H_4 were also shown to involve functional group exchange, and dissociative (reactive) charge transfer, i.e., $O^- + C_2H_4 \rightarrow [OC_2H_4]^{*-} \rightarrow CH_2^- + OCH_2$, and $O^- + C_2H_4 \rightarrow [OC_2H_4]^{*-} \rightarrow CH^- + OCH_3$ (or $\rightarrow CH^- + OCH_2 + H$), respectively; either reaction specifically requires CO bond formation to yield desorbing (i.e. energetic) CH_2^- or CH^-, given the low surface E_k of the O^- formed by DEA to O_2.

Therefore, based on the known average D_o for CH, OH, and CO bonds,[49] and EA[50] for H, O, and OH, here the hydrogen abstraction and atom exchange reactions are believed to explicitly require formation of new bonds, as shown in Scheme 1. Although the excess electron in its diffuse orbital is usually denoted outside the neutral molecular core of the transient collision complex $[OC_4H_8O]^{*-}$, for larger target molecules such as THF it is likely to be more localized near the reaction site, in part due to the high molecular polarizability (8 Å^3) of THF.[51] For example, for reaction 3 we explicitly show hydrogen abstraction at either the α-CH (D_o = 3.98 eV) or β-CH (D_o = 4.12 eV) sites;[49] given the known EA[50] for O (1.46 eV), OH (1.83 eV), and H (0.75 eV) and D_o(OH) = 4.35 eV,[49] reaction 3a is exothermic by 0.74 eV and leads to THF-1(or 4)-yl with the initial radical site on an α-C, while reaction 3b is exothermic by 0.6 eV, and leads to THF-2(or 3)-yl with initial radical site on an β-C. Furthermore, the proximity of the directly attached oxygen heteroatom in THF may also facilitate hydrogen abstraction and radical stabilization; thus, hydrogen abstraction by O^- may be somewhat more likely at the α carbon position. Similarly, we find that H^- formation via direct scattering, reaction 6 in Scheme 1, is endothermic by 4.7−4.83 eV, and thus not accessible to O^- projectiles formed by DEA to O_2 at E(e) below 14 eV.[29] Since the present O^- E_k are well below the first electronic excitation threshold for THF,[31] the dissociative ion reactions observed here will also not involve such excitations. However, if the oxygen projectile becomes bound to, e.g., an α-C during the electron autodetachment lifetime of

the $[OC_4H_8O]^{*-}$ collision complex, with an average CO single bond energy[49] of 4.7−4.1 eV, initial alkoxyl radical and H^- formation via reaction 4 becomes thermoneutral, or endothermic by only 0.57 eV; the latter is well within the range of surface E_k for most O^- formed by DEA to O_2 in the present films, even for E(e) near 5 eV.[29] Alternatively, H^- formation may involve simultaneous formation of a CO double bond (i.e., lactone) at an α-C, and additional free H, viz., reaction 5 in Scheme 1; in that case, using an average $D_o \approx 7.7$ eV[49] of CO double bonds in ketones, aldehydes, esters, and amides, reaction 5 is endothermic by about 1 eV.[52] On the basis of ESD measurements[29] of DEA O^- E_k distributions, this is well within the range of surface E_k(mp) of all O^- formed at E(e) > 7 eV, and surface E_k(max) of most O^- formed at E(e) > 5.5 eV. We note that both, formation of sugar−oxyl-type radicals[53] leading to strand breakage, and C1′ centered sugar−lactones[54] leading to base release, as well as other sugar oxidation products,[30] have been observed in irradiated DNA.

Although not directly observable in our experiments at this time, associative electron detachment (AED, reaction 7) is also included in Scheme 1 for completeness, as a possible decay channel of the $[OC_4H_8O]^{*-}$ collision complex; AED has been observed in O^- gas-phase ion scattering[21,43−48] even at thermal energies, as well as in pulse radiolysis experiments on water,[55] and solutions of small organic molecules,[56] where OH^- formation is also observed.[57] We note that AED[21] (a) always results in formation of highly ro-vibrationally excited neutrals, (b) often involves insertion reactions,[47,58] and (c) is more often than not exothermic. For example, AED involving O insertion at an α-CH bond of THF, leading to formation of α-4(or 1)-hydroxy-THF (or a keto precursor of lactone), would be exothermic by about 2−2.3 eV, using average C−OH (3.7−4 eV),and CO−H (3.7 eV) bond energies in phenols and alcohols;[49] similarly large exothermicities have been observed in, e.g., gas-phase O^- AED reactions[47] with CH_4 and C_2H_4.

We find that, while the OH^- yield has the typical double peaked signature (Figure 2a), resembling DEA to O_2 over the entire range of E(e) < 16 eV, but with a slightly higher threshold near 6 eV, the H^- yield (Figure 2b) attributed here to atom exchange via reaction 4 or 5 in Scheme 1 has only one structure near 8 eV, resembling DEA to only the low-energy resonances of O_2 (yielding O^- with lower E_k), including the threshold at 5 eV. This is mainly attributed to the fact that H-abstraction is a fast process (compared to the collision time of 30 to 10 fs/Å, i.e., the time a 1−5 eV O^- spends near a THF), requiring no THF bond rearrangements since the O^- leaves with the H, and can therefore occur over the entire range of the O^- E_k (1−5 eV). Atom exchange, however, is a slower process, since it requires single or double CO bond formation, and associated stabilizing bond rearrangements in the neutral O−THF-type product; therefore, if the O^- E_k is too high, i.e., for E(e) above 10 eV, most of the O^- simply move too fast to become bound to THF. Furthermore, a transient $[OC_4H_8O]^{*-}$ collision complex of a specific symmetry may dissociate toward different asymptotes via several channels, for which the relative probabilities depend on the following:[21] (a) at what internuclear separation the potential energy surfaces (PES) of the incoming and outgoing trajectories, i.e., the manifold of states associated with particular symmetries and dissociation asymptotes, intersect in the autodetaching region, (b) the shape and position of the PES (repulsive or attractive) at their intersection in the autodetaching region, and (c) the electron autodetachment lifetime of a specific collision complex, compared to the time the reactants spend in close proximity of each other. Thus, the different energetic thresholds for OH^- and H^- desorption more likely indicate that, in the autodetaching region, the manifold of states of different symmetries formed during the reaction lie at different energies relative to the two asymptotic dissociation limits for production of these ions.

The above arguments may also relate to the observation that, while H-abstraction by O^- from either the α- or β-CH bonds of THF is exothermic, OH^- desorption is only seen here for E(e) at which reacting O^- have at least about 1.5−1.7 eV at the surface.[29] However, this almost 1 eV difference between O^- (or H^-) and OH^- desorption thresholds will also be determined by (a) repartitioning of the *total* reaction energy (including the center of mass collision energy, E_{cm}) contained in the dissociating $[OC_4H_8O]^{*-}$ collision complex, as well as (b) elastic (i.e., binary recoil) and inelastic collisions of the O^-, H^-, and OH^- within the film, or at the surface, prior to reaction or desorption; thus, the OH^- that actually desorb are likely to have a lower E_k than the initial O^- projectile, and only O^- with a certain minimum E_k may abstract a hydrogen and still have sufficient E_k to scatter (as OH^-) in the film, *and* overcome the E_p of the solid. This is summarized below:

(a) Using a binary collision approximation,[59] the surface kinetic energy of a specific product anion, E_k(ion), formed by the dissociative decay of the transient $[OC_4H_8O]^{*-}$ collision complex (with total mass M, here = 88 amu), relates to the product ion mass, m_{ion}, via

$$E_k(\text{ion}) = \{1-(m_{ion}/M)\} \times \{\Delta_R H + E_{cm} - E^*\} \qquad \text{(i)}$$

Here Δ_RH is the thermodynamic reaction enthalpy, which depends on the differences of EA and D_o of the reactants and products, $E_{cm} = (m_T/M)E_k$, where m_T is the mass of the THF target (72 amu), E_k is the O^- projectile energy[29] at the surface, or in the bulk, and E^* is the internal excitation energy of the products.[60] For dissociation into $OH^- + {}^{\cdot}C_4H_7O$ via reaction 3, $\{1-(m_{ion}/M)\} \approx 0.807$, while for dissociation into $H^- + OC_4H_8O$ via reaction 4, $\{1-(m_{ion}/M)\} \approx 0.99$. In other words, all else being equal, dissociation of a transient $[OC_4H_8O]^{*-}$ in principle favors production of light fragments.

However, the different $\Delta_R H$ and E^* values for the different reactions will greatly affect the anion formation energetics (as will their subsequent scattering in the film prior to desorption). For example, using eq i with $E^* = 0$ and a surface E_k of 1 eV, an O^- reaction with THF will yield $E_k(OH^-) \approx 1.25$ eV, using the $\Delta_R H \approx 0.74$ eV calculated above and $E_k(H^-) \approx 0.82$ eV, assuming formation via reaction 4 is thermoneutral; both values are larger than the average E_p (≈0.7 eV) needed to desorb. Thus, the 1 eV O^-, produced by DEA at an E(e) near 5.5 eV, should produce OH^- that are as likely to desorb as the H^-. However, considering general gas-phase anion reaction dynamics,[21,44−48,58] we find that here OH^- production via H-abstraction from hydrocarbons will lead to repartitioning of some of the total reaction energy into internal ro-vibrational excitation ($E^* > 0$) of both the OH^- *and* neutral molecular dissociation fragments; this will reduce the OH^- kinetic energy upon formation, while no energy will be repartitioned into E^* of the atomic H^- reaction product.

(b) Most importantly, as known from low-energy ion transmission through condensed films[28] and classical mechanics, even in single binary[59] elastic recoil collisions prior to desorption, at the surface or in the film bulk, the OH^- (17 amu) will suffer significantly greater energy losses than the H^- in collisions with THF (72 amu) or O_2 (32 amu): for projectile scattering angles of 90°, the final energy of the projectile is $E_f = \{(m_T - m_P)/M\}E_i$, where E_i is the initial projectile E_k, m_T

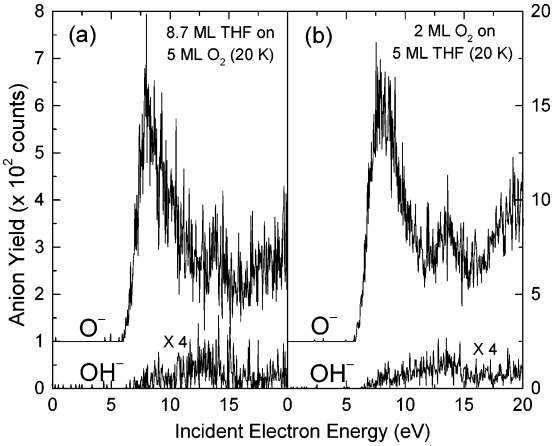

Figure 5. ESD yields of O^- and OH^- as functions of incident electron energy (0−20 eV) from (a) an 8.7-ML film of THF condensed at 20 K on an amorphous/*nonporous* 5-ML film of O_2, also prepared at 20 K, and (b) 2 ML of O_2 dosed at 20 K onto a 5-ML film of amorphous/*porous* THF, also prepared at 20 K. The O^- yields have been vertically displaced for clarity, and the OH^- yields were multiplied by 4.

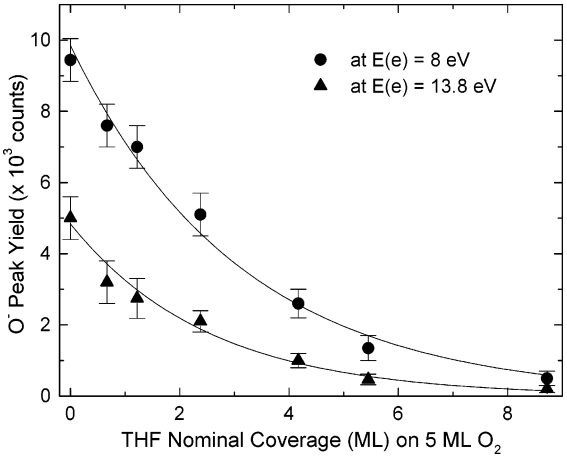

Figure 6. Attenuation of the desorbing O^- DEA yields in THF overlayers, obtained from 5-ML films of O_2 (at 20 K) covered with increasing amounts of THF, at incident electron energies of 8 and 13.8 eV. The curves through the data are exponential fits; see text.

and m_P the target and projectile mass ($m_T > m_P$), and M the total mass of the collision system. Thus, a 1.25 eV OH^- will lose about 40% or 70% of its energy in a single recoil collision with a THF or O_2, respectively, while the 0.82 eV H^- will lose less than 6% in either collision. Consequently, most of the OH^- formed at very low E(e) will not desorb, even after only one recoil collision (more energy will be lost in inelastic collisions involving ro-vibrational excitations of the projectile or target), while an H^- may still desorb, possibly even after several recoil collisions. Furthermore, due to its small mass, H^- collisions in the films are not likely to result in ro-vibrational excitations. This may also explain the intensity difference between the H^- yield produced below 10 eV via reaction 4 or 5 and the OH^- yield produced by reaction 3.

Here, OH^- are not observed to desorb for E(e) significantly below 6 eV, i.e., where the initial O^- E_k(mp) at the surface is near 1.5 eV, and should result in OH^- formation via reaction 3 with average surface $E_k(OH^-)$ near 1.6 eV prior to desorption (using eq i with $E^* = 0$). Since desorption only requires $E_k(OH^-) > E_p \approx 0.7-1$ eV (the latter value is for hydrocarbon solids[20]), this suggests that these OH^-, if formed, may have lost up to 0.6−0.9 eV due to the combined effects of E^*, and scattering losses, and are thus not able to desorb. This is reasonable since a 1.6 eV OH^- can already lose 0.6 or 1.1 eV in a single recoil scattering event with THF or O_2, respectively.

O^- Attenuation and Film Morphology. Shown in Figure 5 are the O^- and OH^- ESD yields for either (a) 8.7 ML of THF condensed at 20 K on 5 ML of nonporous amorphous O_2 or (b) 2 ML of O_2 adsorbed at 20 K on 5 ML of THF, which was also prepared at 20 K and is of amorphous porous structure.[41] We find that even for large amounts of THF condensed on O_2, measurable yields of O^- and OH^- can still be observed with their typical E(e) dependent desorption signatures (but somewhat smeared out, likely due to EEL prior to DEA to O_2, and ion scattering energy losses before desorption), but with their intensities greatly reduced compared to 0.6 ML of THF on 5 ML of O_2 (Figure 2a). Similarly, the O^- and OH^- intensities in Figure 5b, obtained from 2 ML of O_2 deposited on 5 ML of porous amorphous THF, are significantly smaller that those obtained, under otherwise identical conditions, from 5 ML of pure O_2 in Figure 2a (even when differences in total quantity of O_2 are accounted for), or from similar thicknesses of pure O_2 films adsorbed on crystalline hydrocarbon films,[41] and only twice as intense as the equivalent yields observed in Figure 5a. This indicates that in Figure 5b much of the O^- originates within the porous THF film, which has been shown to be due to the fact that O_2, dosed on amorphous porous hydrocarbon films, will diffuse into the pores, with only a small amount remaining at the vacuum-solid interface.[41] Only when sufficient amounts of O_2 have been adsorbed, i.e., when the pores have been filled, and O_2 begins to accumulate at the surface, will the O^- ESD yield intensity begin to resemble that from a pure O_2 film. Thus, the OH^- yield observed in Figure 5b is believed to involve the following: (a) most of the O^- originates within the film and, on a trajectory toward the vacuum, scatters from THF in the bulk, or at the surface, and emerges as OH^-, and (b) small amounts of O^- are formed at the film surface and react with THF prior to desorption as OH^-.

The notion that O^- formed deep within the film is able to scatter through a THF overlayer is supported by the results in Figure 6, which shows the attenuation of O^-, formed by DEA to O_2 near 8 and 13.8 eV, as a function of THF coverage[61] on a 5-ML film of O_2. We find that O^-, formed by DEA to either resonances, is attenuated in the THF overlayers exponentially. As shown elsewhere in low-energy cation/anion transmission experiments through physisorbed rare gas and water overlayers,[28] the exponential dependence of the transmitted ion intensity on overlayer coverage indicates that here the projectile O^- is attenuated by a sequence of successive binary collisions, which either destroy the projectile or change its trajectory.

Thus, assuming random orientation of molecules in the THF overlayer, attenuation of O^- can be modeled by a statistical expression (i.e., Lambert−Beer law) as $I(O^-) = I_o(O^-) \exp[-\rho L\sigma]$, where $I_o(O^-)$ is the initial O^- intensity without THF coverage, $I(O^-)$ is the O^- intensity at a distance L in the film, and ρ is the number density of THF in the overlayer. σ is the attenuation cross section, and includes all mechanisms that either change the trajectory of the O^-, e.g., toward the metal substrate where they are neutralized, or effectively "destroy" the initial target via, e.g., reactions 3−7, as well as direct collisional electron detachment, which becomes energetically allowed at $E_k > EA(O)$.[21] Since our yield functions are angle integrated over a cone subtending a solid angle of 50°, centered on the surface normal,[29a] the O^- attenuation cross section may be roughly estimated from exponential fits to the data by assuming uniform distribution of scattering angles. In that case, given the known density of about 8×10^{21} THF cm^{-3}, and an estimated thickness of about 2.5 Å/ML,[62] σ is about 16 and 20 $Å^2$ at 8

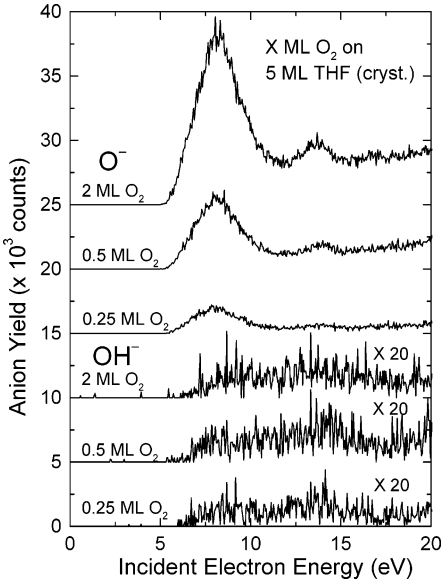

Figure 7. ESD yields of O^- and OH^- from varying amounts of O_2 condensed at 20 K on 5-ML films of crystalline THF, prepared at 80 K, all as functions of incident electron energy (0−20 eV). The yield curves have been vertically displaced for clarity, and the OH^- yields have been multiplied by 20. Other than O_2 overlayer thickness, all experimental conditions were identical.

and 13.8 eV (electron energy), respectively, which is of the order of the geometrical size of the THF. Similar attenuation cross sections in the 10's of Å^2 range have been obtained for transmission of 5−7 eV O^+ through rare gas and NH_3 overlayers, 4 eV F^+ through rare gas layers, and 1 eV F^- through water films.[28]

While the relative contributions of reactions 3−5 to the O^- attenuation are not known, we note that OH^- yields are relatively small compared to the O^- yields, while the H^- yields attributed to reactions 4 and 5 are larger than the OH^- yields; this may imply different cross sections either for these processes or for subsequent scattering prior to desorption. Also, the attenuation cross section of O^- formed near $E(e) = 14$ eV is somewhat larger than that of O^- formed at 8 eV; this is likely due to the higher average $E_k >$ EA(O) (≈1.5 eV) of O^- formed near 14 eV, and above, which allows more projectile destruction, e.g., via direct collisional electron detachment.[21] In any case, we find that almost 9 ML (or about 2.5 nm of THF) are needed to attenuate 95% of the O^-, at which point the OH^- yield is reduced by about 67% of its value compared to sub-ML coverages of THF. This suggests that either some of the 1−5 eV O^- are able to scatter over distances comparable to the diameter of double stranded DNA, and then react near the surface, or some of the OH^-, produced somewhere along the O^- trajectory in the film, are able to scatter somewhat smaller distances.

Finally, the results shown in Figure 7 demonstrate the effect of THF morphology on O^- and OH^- desorption: here increasing amounts of O_2 have been adsorbed at 20 K on a 5 ML thick THF film that was prepared near 80 K and cooled to 20 K; from previous work it is known that this procedure produces crystalline or at least nonporous amorphous hydrocarbon films.[41] Thus, here the O_2 are expected to remain at the surface of the film, with the effect that for 2 ML of O_2 on 5 ML of crystalline THF (top curve in Figure 7) the O^- yield is significantly larger than that for the same amount of O_2 adsorbed on porous THF, shown in Figure 5b, where most of the O_2 is believed to be located in the pores of the THF film. While these morphology effects on O^- desorption and reaction in THF films are currently under detailed investigation,[63] we briefly note the following general points: (a) The OH^- yield increases for O_2 coverages up to about 1 ML (not shown for clarity), and gradually decreases for higher coverages (up to 2 ML in the present experiments). This indicates that as the O_2 overlayer thickness increases, less OH^-, produced at the O_2−THF interface, will be able to survive backscattering through the film. While the fate of these OH^- is not known here, in the gas phase OH^- reactions with hydrocarbons[48] also lead to hydrogen abstraction, i.e., $OH^- + C_nH_m \rightarrow [HOC_nH_m]^{*-} \rightarrow H_2O + (C_nH_{m-1})^-$ with similarly large cross sections as via O^- reactions. (b) The fact that OH^- is nonetheless observed here suggests that some O^- are able to scatter into the THF layer below, abstract a hydrogen, backscatter as OH^- through the overlayers, and still have enough energy to overcome the charge-induced polarization barrier (surface $E_p \approx 0.7$ eV for O_2) and desorb into the vacuum. (c) The OH^- yield functions still retain their double peaked signature, resembling the formation of the O^- projectile via DEA to O_2, but are smeared out, likely due to EEL prior to O^- formation via DEA to O_2, and O^- (or OH^-) scattering energy losses prior to reaction (or desorption).

Thus, from a purely experimental perspective, for the present O_2−THF system at $E(e) < 20$ eV, both O^- induced H-abstraction from THF (i.e., OH^- formation) and atom exchange reactions are more clearly observable for submonolayer quantities of THF adsorbed on comparably thick O_2 films. This allows for easier penetration of the incident electrons, and less scattering energy losses of the product ions prior to desorption.

Summary and Conclusions

We have presented measurements of O^- reactions in physisorbed films of tetrahydrofuran (THF, C_4H_8O), a DNA sugar analogue, initiated in situ by 0−20 eV electron impact in films containing both THF and O_2. The results show that both hydrogen abstraction (OH^- formation) and reactive charge transfer (atom exchange) are energetically possible for 1−5 eV O^-. These reactions may lead to respectively (a) formation of THF-yl radicals and energetic OH^- or (b) oxygen addition, most likely via alkoxyl or lactone formation at an α-C1(orC4) of THF, where either is associated with formation of a free energetic H^-; however, similar reactions at the β-carbons are also possible, and lactone formation would generate an additional free H radical. Based on comparison with available gas and condensed phase measurements, we propose that here, at the small impact parameters dictated by the condensed phase, the O^- + THF reactions proceed via formation of a $(O-THF)^{*-}$ transition state (or collision complex) that may decay along numerous energetically allowed pathways. Furthermore, from O^- attenuation measurements through THF overlayers up to 2−3 nm thick, we find that 1−5 eV O^- are able to scatter (or react) in THF films over distances comparable to the diameter of double stranded DNA, while hydrogen abstraction yields some OH^- with sufficient energy to scatter in the films and still overcome the charge-induced polarization barrier (0.7−1 eV).

From a radiobiological perspective, our results imply that *similar* nonthermal O^-, formed in DNA by the abundant ballistic secondary electrons via DEA to a base,[7,9] phosphate,[16] or protein,[13,14] may not only result in lethal sugar radicals and oxidation products, but also create OH^- that still have sufficient kinetic energy to contribute to further damage, in addition to that subsequently induced by the remaining sugar radicals. In that sense, the observation of OH^- desorption from plasmid DNA by 1−20 eV electron impact,[16] which is accompanied by resonant formation of DNA single and double strand breaks,[17] may already be the result of such O^- reactions.

We also note the following: (a) In addition to the reactions observed here, gas-phase O^- reactions with hydrocarbons,[48a] mediated by a $[OC_nH_m]^{*-}$ transition state, also lead to formation of $OH^{\cdot} + (C_nH_{m-1})^-$, with high reaction rates; *double* H-abstraction by O^- from some alcohols,[57,64] or benzidine,[65] viz., $O^- + C_nH_m \rightarrow [OC_nH_m]^{*-} \rightarrow H_2O + (C_nH_{m-2})^-$, has also been observed in pulse radiolysis measurements. While such heavy anion products are not sufficiently energetic to overcome the E_p in the present experiments, their formation would be quite exothermic, and should therefore not be ruled out here. (b) AED, i.e., reaction 7 in Scheme 1, is usually exothermic whenever the projectile EA is less than the energy of the new bond(s) formed[21] (as is the case here), resulting in oxidized products in solutions[55,56] *and* the gas phase,[45−48] and often involves insertion reactions.[45−48,58] Thus, while our present experimental methods prevent their detection at this time, AED reaction products, such as α-4-hydroxy-THF, or similar THF-hydroxy analogues, are highly likely to be formed here as well.

In irradiated DNA, the formation of similar deoxyribose lesions, or sugar analogues of the products proposed here (Scheme 1), are known to involve H-abstraction (by OH radicals) from either of the five carbon positions in deoxyribose, followed by oxidation and fragmentation; this leads to various types of lethal clustered lesions,[30,66] and DNA−protein cross links. In the latter experiments deoxyribose damage by ionizing radiation always involves complex sequences of thermal reactions; however, the present experiments provide evidence for an alternative *nonthermal* reaction mechanism, involving the ballistic radical O^- that are known to be formed in DNA,[16] or its components,[7,9,13,14] by the 1−20 eV secondary electrons that are ubiquitous in irradiated media. Furthermore, since in our experiments the reactive O^- originate from secondary electron attachement (DEA) to O_2, the present results may also be relevant to sugar damage pathways observed elsewhere in irradiated DNA under aerobic conditions.[66a]

Much like molecular excitation or ionization, the *fundamental* ion reactions reported here are generally observed, or observable, in any molecular system (however, somewhat modulated by the particular physical and chemical nature of the target). Thus, they are expected to occur in living cells as well, and a full understanding of the biological effects of ionizing radiation must incorporate a detailed knowledge of the nascent ion and radical reaction cascades induced along radiation tracks.

Acknowledgment. This work was supported in part by individual research grants from the Canadian Institutes of Health Research (L. Sanche and M. A. Huels) and the Natural Science and Engineering Research Council of Canada (M. A. Huels). M.A.H. also wishes to thank Christiane Collins (MIT Dedon Group) for valuable discussions on sugar oxidation products and pathways in DNA.

References and Notes

(1) *ICRU Report 31*; International Commission on Radiation Units and Measurements: Washington, DC, 1979. *ICRU Report 55*; International Commission on Radiation Units and Measurements: Washington, DC, 1995.

(2) Pimblott, S. M.; LaVerne, J. A. In *Radiation Damage in DNA*: *Structure/Function Relationships at Early Times*; Fuciarelli, A. F., Zimbrick, J. D., Eds.; Battelle Press: Columbus OH, 1995; Chapter 1. LaVerne, J. A.; Pimblott, S. M. *Radiat. Res.* **1995**, *141*, 208.

(3) Cobut, V.; Frongillo, Y.; Patau, J. P.; Goulet, T.; Fraser, M.-J.; Jay-Gerin, J.-P. *Radiat. Phys. Chem*. **1998**, *51*, 229.

(4) For reviews see: *Electron−Molecule Interactions and Their Applications*; Christophorou, L. G., Ed.; Academic Press: Orlando, FL, 1984; Vol. 1. Sanche, L. *Scanning Microsc.* **1995**, *9*, 619.

(5) Even in experiments on "dry" DNA films, the minimum water content amounted to about 2.5 water molecules per base pair; see, for example: Swarts, S. G.; Sevilla, M. D.; Becker, D.; Tokar, C. J.; Wheeler, K. T. *Radiat. Res.* **1992**, *129*, 333. Furthermore, in cells, hydrated DNA is impacted in the nucleosome together with proteins; thus, water *and* amino acids should also be considered to be fundamental components (or subunits) of realistic cellular DNA.

(6) (a) Antic, D.; Parenteau, L.; Lepage, M.; Sanche, L. *J. Phys. Chem. B* **1999**, *103*, 6611. (b) Antic, D.; Parenteau, L.; Lepage, M.; Sanche, L. *J. Phys. Chem. B* **2000**, *104*, 4711.

(7) Huels, M. A.; Hahndorf, I.; Illenberger, E.; Sanche, L. *J. Chem. Phys.* **1998**, *108*, 1309.

(8) Hervé du Penhoat, M.-A.; Huels, M. A.; Cloutier, P.; Jay-Gerin, J.-P.; Sanche, L. *J. Chem. Phys.* **2001**, *114*, 5755.

(9) Abdoul-Carime, H.; Cloutier, P.; Sanche, L. *Radiat. Res.* **2001**, *155*, 625.

(10) Abouaf, R.; Pommier, J.; Dunet, H. *Int. J. Mass Spectom.* **2003**, *226*, 397.

(11) Hanel, G.; et al. *Phys. Rev. Lett.* **2003**, *90*, 188104-1.

(12) Rowntree, P.; Parenteau, L.; Sanche, L. *J. Chem. Phys.* **1991**, *94*, 8570.

(13) Gohlke, S.; Rosa, A.; Illenberger, E.; Brüning, F.; Huels, M. A. *J. Chem. Phys.* **2002**, *116*, 10164.

(14) (a) Abdoul-Carime, H.; Cecchini, S.; Sanche, L. *Radiat. Res.* **2002**, *158*, 23. (b) Abdoul-Carime, H.; Sanche, L. *Radiat. Res.* **2003**, *160*, 86.

(15) (a) Dugal, P.-C.; Huels, M. A.; Sanche, L. *Radiat. Res.* **1999**, *151*, 325. (b) Abdoul-Carime, H.; Dugal, P.-C.; Sanche, L. *Radiat. Res.* **2000**, *153*, 23. (c) Dugal, P.-C.; Abdoul-Carime, H.; Sanche, L. *J. Phys. Chem. B* **2000**, *104*, 5610.

(16) Pan, X.; Cloutier, P.; Hunting, D.; Sanche, L. *Phys. Rev. Lett.* **2003**, *90*, 208102-1.

(17) (a) Boudaïffa, B.; Cloutier, P.; Hunting, D.; Huels, M. A.; Sanche, L. *Science* **2000**, *287*, 1658. (b) Huels, M. A.; Boudaiffa, B.; Cloutier, P.; Hunting, D.; Sanche, L. *J. Am. Chem. Soc.* **2003**, *125*, 4467.

(18) Caron, L. G.; Sanche, L. *Phys. Rev. Lett.* **2003**, *91*, 113201-1.

(19) The lowest IPs of DNA components are found near 8 eV for guanine (Sevilla, M. D.; Besler, B.; Colson, A.-O. *J. Phys. Chem.* **1995**, *99*, 1060), 6.5 eV for a stacked GC base pair, 5.7 eV for a fully "solvated" GC base pair (Colson, A.-O.; Besler, B.; Sevilla, M. D. *J. Phys. Chem.* **1993**, *97*, 13852), and 10−11 eV for B and Z sugar−phosphate backbone fragments (Colson, A.-O.; Besler, B.; Sevilla, M. D. *J. Phys. Chem.* **1993**, *97*, 8092). Thus, the a priori minimum energy for two ionizations to occur on a fully solvated GC pair would be 2×5.7 eV; since delocalization of the two holes on the base pair may not necessarily lead to a double strand break, i.e., two SSBs on opposing phosphate−sugar backbones, the minimum energy for two ionizations (SSBs) on opposing backbones would be more near 2×10 eV.

(20) Sanche, L.; Parenteau, L. *J. Chem. Phys.* **1990**, *93*, 7476.

(21) For reviews see: (a) Massey, H. S. W. *Negative Ions*, *Cambridge Monographs on Physics*; Woolfson, M. M., Ziman, J. M., Eds.; Cambridge University Press: Cambridge, UK, 1976; Chapters 12−15. (b) *Gas-Phase Ion Chemistry*; Bowers, M. T., Ed.; Academic Press: New York, 1979; Vol. 1. (c) Champion, R. L.; Doverspike, L. D. In *Electron−Molecule Interactions and Their Applications*; Christophorou, L. G., Ed.; Academic Press: Orlando, FL, 1984; Vol. 1, Chapter 7, and references therein.

(22) Sanche, L.; Parenteau, L. *Phys. Rev. Lett.* **1987**, *59*, 136.

(23) Bass, A. D.; Parenteau, L.; Huels, M. A.; Sanche, L. *J. Chem. Phys.* **1998**, *109*, 8635.

(24) Huels, M. A.; Parenteau, L.; Sanche, L. *Chem. Phys. Lett.* **1997**, *279*, 223.

(25) Azria, R.; Parenteau, L.; Sanche, L. *Chem. Phys. Lett.* **1990**, *171*, 229.

(26) Kimmel, G. A.; Orlando, T. M.; Vézina, C.; Sanche, L. *J. Chem. Phys.* **1994**, *101*, 3282.

(27) Cobut, V.; Jay-Gerin, J.-P.; Frongillo, Y.; Patau, J. P. *Radiat. Phys. Chem.* **1996**, *47*, 247.

(28) Akbulut, M.; Sack, N. J.; Madey, T. *Surf. Sci. Rep.* **1997**, *28*, 177.

(29) (a) Huels, M. A.; Parenteau, L.; Michaud, M.; Sanche, L. *Phys. Rev. A* **1995**, *51*, 337. (b) Huels, M. A.; Parenteau, L.; Sanche, L. *Phys. Rev. B* **1995**, *52*, 11, 343. (c) Azria, R.; LeCoat, Y.; Ziesel, J. P.; Guillotin, J. P.; Mharzi, B.; Tronc, M. *Chem. Phys. Lett.* **1994**, *220*, 417. (d) Azria, R.; Parenteau, L.; Sanche, L. *Phys. Rev. Lett.* **1987**, *59*, 638.

(30) von Sonntag, C. *The Chemical Basis for Radiation Biology*; Taylor and Francis: London, UK, 1987.

(31) Near-threshold electron energy loss spectra for gas-phase THF show evidence of three low-lying absorption bands which are assigned to excitations of Rydberg states $^1n_o3s$, $^1n_o3p$, $^1n_o3d$, with maxima near 6.6, 7.2, and 7.8 eV, respectively; the excited state at 6.6 eV may also contain a valence excitation. See: (a) Bremner, L. J.; Curtis, M. G.; Walker, I. C. *J. Chem. Soc., Faraday Trans.* **1991**, *87*, 1049−1055. (b) Tam, W.-C.; Brion, C. E. *J. Electron Spectrosc. Relat. Phenom.* **1974**, *3*, 263−279.

(32) Huels, M. A.; Parenteau, L.; Sanche, L. *J. Chem. Phys.* **1994**, *100*, 3940.

(33) Gaubert, C.; Baudoing, R.; Gauthier, Y.; Michaud, M.; Sanche. L. *Appl. Surf. Sci.* **1986**, *25*, 195.

(34) Sanche, L. *J. Chem. Phys.* **1979**, *71*, 4860.
(35) Sanche, L.; Deschêne, M. *Phys. Rev. Lett.* **1988**, *61*, 2096.
(36) Sanche, L. *Phys. Rev. Lett.* **1984**, *53*, 1638.
(37) The relaxation of the $\Sigma^- \not\leftrightarrow \Sigma^+$ gas-phase selection rule is attributed to the breaking of the cylindrical symmetry of the molecular wave function by adjacent molecules in the condensed films. See ref 29c.
(38) These multiple scattering electron energy losses (EEL) in O_2 films (followed by DEA to the $^2\Pi_u$ and $^2\Sigma_g^+$(I) resonances) mainly involve excitations of A $^3\Sigma_u^+$, C $^3\Delta_u$, c $^1\Sigma_u^-$, and the Schumann−Runge continuum, and have been shown to dominate the ESD O^- yields and kinetic energy distributions above 12 eV—see ref 29a. This is supported by measurements of the O^+ ESD yield thresholds in O_2 films (from DD to O_2: Huels, M. A.; Sanche, L. unpublished) which lie near 18 eV; thus, most of the monotonically rising O^- signal above 11 eV (top curve in Figure 2a) is attributed to EEL followed by DEA.
(39) Sanche, L.; Bass, A. D.; Ayotte, P.; Fabrikant, I. I. *Phys. Rev. Lett.* **1995**, *75*, 3568 and references therein.
(40) Hedhili, M. N.; Parenteau, L.; Huels, M. A.; Azria, R.; Tronc, M.; Sanche, L. *J. Chem. Phys.* **1997**, *107*, 7577.
(41) See: Bass, A. D.; Parenteau, L.; Weik, F.; Sanche, L. *J. Chem. Phys*. **2001**, *115*, 4811 and references therein.
(42) This is generally observed here, and is mainly due to different EEL effects in the THF overlayer prior to DEA to O_2, and other extrinsic film effects on DEA and DD, discussed elsewhere: Huels, M. A.; Parenteau, L.; Sanche, L. *J. Chem. Phys.* **1994**, *100*, 3940.
(43) See: Huq, M. S.; Doverspike, L. D.; Champion, R. L. *Phys. Rev.* **1983**, *A27*, 785 and references therein.
(44) Ramond, T. M.; et al. *J. Phys. Chem.* **2002**, *106*, 9641.
(45) Comer, J.; Schulz, G. L. *Phys. Rev.* **1974**, *A10*, 2100.
(46) Parkes, D. A. *J. Chem. Soc., Faraday Trans.* **1972**, *I68*, 613.
(47) Lindinger, W.; Albritton, D. L.; Fehsenfeld, F. C.; Fergusson, E. E. *J. Chem. Phys.* **1975**, *63*, 3238.
(48) See, e.g.: (a) Bohme, D. K.; Young, L. B. *J. Am. Chem. Soc.* **1970**, *92*, 3301. (b) Bohme, D. K.; Fehsenfeld, F. C. *Can. J. Chem.* **1969**, *47*, 2717. (c) Albritton, D. L. *At. Data Nucl. Data Tables* **1978**, *22*, 1.
(49) Unless otherwise indicated, all bond dissociation energies (D_o) used here are found in: (a) Yu-Ran, L. *Handbook of Bond Dissociation Energies in Organic Compounds*; CRC Press: Boca Raton, FL, 2003. (b) Lide, D. R.; *Handbook of Chemistry and Physics*, 82nd ed.; CRC Press: Boca Raton, FL, 2001. (c) Vollhardt, K. P. C.; Schore, N. E. *Organic Chemistry—Structure and Function*, 3rd ed.; W. H. Freeman and Co.: New York, 2000. (d) Herzberg, G. *Molecular Spectra and Molecular Structure*, 2nd ed.; Van Nostrand Reinhold Co.: New York, 1950.
(50) All electron affinities (EA) are from: Janousek, B. K.; Brauman, J. I. Electron Affinities. In *Gas-Phase Ion Chemistry*; Bowers, M. T., Ed.; Academic Press: New York, 1979; Vol. 2, Chapter 10.
(51) Estimated using free web-access software: Gasteiger, J. *Parameter Estimation for the Treatment of Reactivity Applications (PETRA)*; Universität Erlangen: Erlangen, Germany (http://www2.chemie.uni-erlangen.de/services/petra/index.html). This software allows parameter estimation of various molecular properties, including bond energies and polarizabilities, for many small organic compounds (but not small inorganic species), with reasonable accuracy; however, here they are only used to estimate *trends* in bond energies, and bond or charge rearrangements due to atom abstraction or replacement, rather than to provide precise values.
(52) For reactions 4 and 5, concerted bond rearrangements in the THF−alkoxyl or THF−lactone may lower these endothermicities, e.g., THF−alkoxyl formation at α-C1 may be associated with reductions in bond energies between α-C1 and *β*-C2, α-C1 and the adjacent O heteroatom, and α-C1 and H (estimated trends using PETRA, ref 51).
(53) Dizdaroglu, M.; Schulte-Frohlinde, D.; von Sonntag, C. *Z. Naturforsch., C* **1975**, *30*, 826.
(54) Dizdaroglu, M.; Schulte-Frohlinde, D.; von Sonntag, C. *Int. J. Radiat. Biol.* **1977**, *32*, 481.
(55) E.g., see: (a) Hickel, B.; Sehsted, K. *J. Phys. Chem.* **1991**, *95*, 744. (b) Matheson, M. S.; Rabani, J. *J. Phys. Chem.* **1965**, *69*, 1324.
(56) In many of these cases, AED, viz., $O^- + M \rightarrow {}^{\cdot}OM + e^-$, is followed by H abstraction from the water solvent by the newly formed oxide, leading to final M−OH formation, e.g., O^- + aniline: (a) Qin, L.; Tripathi, G. N. R.; Schuler, R. H. *Kosmophys.* **1985**, *40A*, 1026. (b) Neta, P.; Schuler, R. H. *Radiat. Res.* **1975**, *64*, 233. (c) Christensen, H. *Int. J. Radiat. Phys. Chem.* **1972**, *4*, 311. O^- + cytosine: (d) Hissung, A.; von Sonntag, C. *Z. Naturforsch., B* **1978**, *33B*, 321.
(57) Most notable examples for OH^- formation by H abstraction in O^- reactions observed in liquid radiolysis are: (a) Solar, S.; Getoff, N.; Sehsted, K.; Holcman, J. *Radiat. Phys. Chem.* **1993**, *41*, 825 (for O^- + 3-methylpyridine). (b) Soeylemez, T.; Schuler, R. H. *J. Phys. Chem.* **19745**, *78*, 1052 (for O^- + cyclopentene). (c) Neta, P.; Schuler, R. H. *J. Phys. Chem.* **1975**, *79*, 1 (for O^- + allylbenzene). (d) Sehsted, K.; Holcman, J. *Nukleonica* **1979**, *24*, 941 (for O^- + ethylbenzene). For more literature on O^- reactions leading to H abstraction or AED, see data compilations at the University of Notre Dame, IN, available at http://www.rcdc.nd.edu.
(58) See, e.g.: Huq, M. S.; Scott, D.; Champion, R. L.; Doverspike, L. D. *J. Chem. Phys.* **1985**, *82*, 3118.
(59) A gas-phase-like binary collision approximation, based on energy and momentum conservation, is used here, because (a) in the present dielectric physisorbed systems (cryogenic, van der Waals solids) the molecular binding energies (10−100 meV range) are much smaller than the average O^- projectile E_k(1−5 eV) and (b) typical periods for lattice vibrations (10^{-13} s) are larger than the average collision times (10^{-14} s) (see refs 28 and 29a for detailed discussions). For projectile E_k *significantly* below 1 eV, this approximation is no longer valid; however, for $E_k < 0.7$ eV $\approx E_p$ no ions desorb, and the present approximation is believed to be valid for the initial O^- + THF collisions in the films.
(60) Here, for reactions 3−6 in the condensed phase, effects of E_p on the reaction/dissociation dynamics can be neglected, since all involved states, i.e., the initial [O^- + THF], transient [OC_4H_8O]* $^-$, and final [OH^- + THF-yl] or [H^- + THF-alkoxyl], are anionic states, that are equally affected by the E_p of the surrounding medium. This is different from DEA (neutral to anion state transition—see ref 29a,b) or AED (anion to neutral state transition).
(61) Some THF mixing with O_2 may occur for about the first ML of THF, based on previous studies of ion scattering in physisorbed films (refs 28 and 23), and physisorption kinetics considerations (Hudson, J. B. *Surface Science*: *An Introduction*; Butterworth-Heinemann: Stoneham, MA, 1992).
(62) Based on the known density of about 0.89 g cm^{-3} for liquid THF (ref 49b) and the approximate size of THF (from average bond distances and angles; ref 49c) estimated to be about $5 \times 4 \times 2$ Å^3.
(63) Mozejko, P.; Parenteau, L.; Sanche, P. To be submitted for publication).
(64) Eliot, A. J.; McCracken, D. R. *Radiat. Phys. Chem.* **1989**, *33*, 69.
(65) Dey, G. R.; Naik, D. B.; Kishore, K.; Moorthy, P. N. *Radiat. Phys. Chem.* **1994**, *43*, 481.
(66) See, e.g.: (a) Knapp-Pogozelski, W.; Tullius, D. *Chem. Rev.* **1998**, *98*, 1089. (b) Balasubramanian, B.; Knapp-Pogozelski, W.; Tullius, D. *Proc. Natl. Acad. Sci.* **1998**, *95*, 9738. (c) Hashimoto, M.; Greenberg, M. M.; Kow, Y. W.; Hwang, J.-T.; Cunningham, R. P. *J. Am. Chem. Soc.* **2001**, *123*, 3161. (d) Roupioz, Y.; Lhomme, J.; Kotera, M. *J. Am. Chem. Soc.* **2002**, *124*, 9129. (e) Collins, C.; Awada, M. M.; Zhou, X.; Dedon, P. C. *Chem. Res. Toxicol.* **2003**, *16*, 1560.